J. Synchrotron Rad. (1996). **3**, 213–219

PIN Silicon Diodes as EXAFS Signal Detectors

G. Dalba,[a] P. Fornasini,[a] Y. Soldo[a]† and F. Rocca[b]

[a]Istituto Nazionale di Fisica della Materia, Dipartimento di Fisica, Università degli Studi di Trento, Via Sommarive 14, 38050 Povo (Trento), Italy, and [b]CeFSA, Centro CNR di Fisica degli Stati Aggregati, 38050 Povo (Trento), Italy

(*Received 31 January 1996; accepted 8 May 1996*)

The properties of PIN silicon diodes as X-ray detectors for EXAFS measurements with synchrotron radiation have been investigated. Electronic stability, linearity and noise current have been analyzed. The effects of diffraction peaks resulting from the crystalline nature of the diodes have been minimized by mounting the diodes on a simple device that continuously changes its orientation by a few degrees with respect to the X-ray beam. An accurate comparison between EXAFS signals monitored by ionization chambers and PIN photodiodes is presented. It is shown that good-quality EXAFS measurements with PIN photodiodes are possible if diffraction effects are eliminated.

Keywords: EXAFS detectors; PIN silicon diodes; X-ray absorption spectroscopy.

1. Introduction

Third-generation synchrotron radiation sources are characterized by high photon fluxes and high brilliancies. Thus, for example, a second-generation source such as the SRS at Daresbury (UK) can reach a brilliance of 10^{13} photons s^{-1} $mrad^{-2}$ mm^{-2} (0.1% bandwidth)$^{-1}$ at the 5 T wiggler beamline, whereas the new European facility, the ESRF in Grenoble, can reach a brilliance of *ca* 10^{17} photons s^{-1} $mrad^{-2}$ mm^{-2} (0.1% bandwidth)$^{-1}$ at an undulator beamline.

Such high-brilliance photon beams require new types of detectors, able to avoid saturation problems (Goulon, 1991). In EXAFS experiments, ionization chambers are commonly used as detectors. They present many advantages, such as good linearity and efficiency in a wide energy range; furthermore, the X-ray absorption efficiency can be optimized as a function of photon energy by changing the type and/or the pressure of the filling gas. The disadvantages of ionization chambers are microphonic noise and, in the presence of high fluxes, saturation. The upper limit for the measurable photon flux depends on the possibility of collecting all the ionized atoms on the electrodes of the chamber. The maximum current per unit surface area which can be collected by the electrodes of an ionization chamber in the linear regime (Wilkinson, 1950) is

$$i = 9\varepsilon_0 \mu V^2 / l^3, \qquad (1)$$

where i is measured in A m^{-2}, μ is the ion mobility, l the distance between the electrodes, V the applied potential, and ε_0 the permittivity of a vacuum (SI units).

For instance, at the bending-magnet beamline D8 (GILDA) of the ESRF a total flux of *ca* 10^{12} photons s^{-1} at 20 kV of photon energy is expected to be focused on 1 mm^2 of sample. The corresponding current in an ionization chamber filled with krypton at 1 bar pressure would be *ca* 0.14 mA. By considering a minimum gap of 1 cm between the electrodes, a maximum accelerating voltage of 500 V and an average horizontal beam size of 2 cm in the electrode region, the chamber should be 2.3 m long to absorb the high photon flux whilst avoiding saturation. Such a long chamber would present mechanical problems of stability and large microphonic noise.

The limits of performance of ionization chambers might be reached at most of the ESRF beamlines. New alternative detectors for EXAFS signals should be characterized by high efficiency in a wide energy range, good linearity, good signal-to-noise ratio and should not saturate (Goulon, 1991).

The use of PIN diodes as EXAFS detectors has been investigated previously (Bouldin, Forman & Bell, 1987; Storb, Dedek, Weber & Lengeler, 1991; Lagarde, Lemonnier & Dexpert, 1989): their advantages are high response (about ten times higher than ionization chambers), vacuum and cryogenic compatibility, no microphonic noise, good linearity, wide dynamic range, very simple electronics, and low cost.

Linearity tests on silicon PIN (*ca* 500 μm thick) and GaAs Schottky diodes from different manufacturers (Ame, Centronics, Hamamatsu and Siemens) have already shown high dynamical range and linearity within ± 0.3% over at least five decades at 20 keV (Storb *et al.*, 1991). PIN diodes (Bouldin *et al.*, 1987) were tested as constant-energy fluorescence detectors and compared with gas-filled chambers, although no quantitative analysis of measured spectra was presented. Diodes were also checked in EXAFS experiments to monitor the transmitted photon flux as a function of energy, but in this case the signal was affected by non-negligible distortions due to Bragg diffraction within the

† Present address: CNRS, Laboratoire de Cristallographie, 25 avenue des Martyrs, Grenoble, France.

ISSN 0909-0495

diode. In fact, at particular energies and orientations the beam is diffracted by crystallographic planes of the diode giving rise to sharp changes of the transmitted signal.

The present paper shows how photodiodes can be conveniently used as detectors for EXAFS measurements. Attention is focused on the elimination of the effects of Bragg reflections, obtained by mounting the diode on a special device which continuously changes its orientation with a frequency of a few Hz. The idea of decreasing Bragg reflections by a continuous movement of the diffracting material is not new: for example, it has been applied to study single crystals by EXAFS in fluorescence configuration (Pant & Hayes, 1994). In this paper we show that, as a result of the high angular dependence of diffraction phenomena, a precession movement of the diffracting crystal (even of a few degrees) is sufficient to average the effect to a negligible value.

Two commercial PIN diodes have been characterized: electronic stability, linearity response, and dark and noise currents have been studied. An accurate comparison between EXAFS signals monitored by ionization chambers and photodiodes is presented.

2. Experimental details

We have tested two commercial PIN diodes: UV-444BQ and YAG-44 produced by EG&G. Both are crystalline silicon diodes, with an effective area of *ca* 10 mm^2 and nominal depletion layers of 300 and 400 μm, respectively, with some differences in the assembly and electrical connections. The choice of these diodes is due to their efficiency, which depends on the thickness of the depletion layer: with a thickness of 400 μm the X-photons are completely absorbed up to *ca* 10 keV, while at 20 keV 33% of the beam is absorbed.

PIN diodes can operate in either photovoltaic and photoconductive mode. In photovoltaic mode no reverse voltage is applied to the diode; the main source of noise is thermal excitation, and no shot noise due to surface and bulk leakage currents is present. In photoconductive mode, in which an external bias with inverse polarization is applied to the diode, a larger frequency response can be achieved, but noise current is also larger owing to both thermal and shot noise. In performing conventional, non-time-resolved EXAFS measurements, we were more interested in reducing the noise current than in increasing the frequency response. For this reason we performed all measurements in photovoltaic mode.

The diodes were mounted inside a metallic cylindrical housing, acting as a Faraday screen; the original glass window was replaced by an aluminium foil a few micrometers thick in order to shield the diode from visible light. In order to reduce diffraction effects we have built a simple system based on a gimbal design similar to that used in gyroscopes, as shown in Fig. 1. The housing was mounted on a ring able to rotate around the horizontal axis φ_1, perpendicular to the beam direction and lying in the plane of the synchrotron; the housing was also allowed to rotate with respect to the ring around the vertical axis φ_2, perpendicular to φ_1. Rocking movement was obtained by connecting the rear of the housing to a rotating eccentric wheel. The centre of the active surface of the photodiode was placed at the intersection of the φ_1 and φ_2 axes. The resulting movement consists of a precession of the vector normal to the surface of the photodiode a few degrees wide: because of the slight looseness of the mechanical connections, some random fluctuations are added to the regular precessional movement.

The maximum noise current measured in the fixed configuration by a digital electrometer (Keithley model 486) set to the lowest scale was 1 pA for UV-444BQ and *ca* 180 pA for YAG-444 (1 pA corresponds to *ca* 2.3×10^3 photons s^{-1} at 10 keV). Data acquisitions performed over long time periods showed stable values of noise current.

Preliminary measurements with synchrotron radiation were made at the PWA laboratory of Adone (Frascati, Italy) in the fixed-diode configuration; the measurements with the rocking diodes and the linearity tests were performed at the SRS at Daresbury (UK). The intensity I_0 of the incoming beam was always measured with an ionization chamber, while the transmitted signal I was measured alternatively with a diode or an ionization chamber. At the SRS both diode and ionization chamber were connected to a current-to-voltage amplifier (Keithley model 428), a voltage-to-frequency converter, a frequency counter and a computer to store the data. The minimum dark current (the current measured by the whole acquisition set-up of the SRS in the absence of the X-ray beam) was *ca* 5 pA with gain 10^9 for UV-444BQ and *ca* 35 pA with gain 10^{10} for YAG-444.

3. Results

3.1. *Linearity tests*

Linearity tests were performed on both diodes at several different X-ray energies. Here we present tests performed at 20 and 25 keV, where the efficiency of the photodiode is strongly reduced by its small thickness. The intensity of the beam was reduced using Cu foils (Goodfellow, 25 ± 2 μm thick). The aim of the experiment was to check the linearity of the relationship between the theoretical transmission coefficient $T = \exp(-n\mu x)$ (where μ is the absorption coefficient of copper, x the nominal thickness of one foil, and n the number of foils) and the experimental ratio I_d/I_0 between the signals of the detectors behind and in front of the absorbers.

At each amplification gain of the electrometers, the dark current (measured current in the absence of X-rays) was subtracted from I_0 and I_d, respectively. The upper limit of the intensity range of the linearity tests at the various energies was set by the initial intensity of the beam. The I_0 current, measured with an ionization chamber filled with 1 bar of argon, varied in the range 9.5–16 nA at 20 keV and 0.7–4.3 nA at 25 keV, in response to electron-beam

attenuation. The current measured by the diodes was in the range 10^{-11}–10^{-6} A.

Our measurements were affected by two types of errors, the first related to current measurements, the second to the thickness of the Cu foils. The uncertainty on the thickness x was $\pm 2\,\mu$m. Owing to these uncertainties, linearity could not be checked for diode currents lower than 10^{-11} A.

Typical results are shown as filled circles in Fig. 2. The vertical error bars take into account uncertainties on both current measurements and foil thickness (Bevington, 1969). Continuous lines are best-fit straight lines $\ln(I_d/I_0) = m(n\mu x) + q$. In every case the χ^2 test guaranteed a linear dependence of $\ln(I_d/I_0)$ on $n\mu x$ with a confidence higher than 99%. The intercept q was checked to be equal to the logarithm of the ratio of signals measured in the absence of Cu foils, $\ln(I_d/I_0)_{n=0}$. These results are summarized in Table 1.

Table 1
Results of the linearity test presented in Fig. 2.

Comparison between the experimental value of the logarithm of the signals in the absence of Cu foils and the q value obtained by the best fit of experimental data. In the last column the probability P for a linear distribution obtained by the χ^2 test is shown.

Diode	Energy (keV)	q	$\ln(I_d/I_0)$	P
UV-444BQ	20	2.09 ± 0.06	2.104	1.00
	25	2.28 ± 0.03	2.258	0.99
YAG-444	20	2.30 ± 0.07	2.278	0.98
	25	2.46 ± 0.03	2.450	0.99

Figure 1
The simple system, based on a gimbal design, used to eliminate the Bragg peaks from the absorption spectra.

The results of linearity tests can be considered satisfactory: in particular, the response of the UV-444BQ diode (showing the lowest noise current) is linear over four orders of magnitude at 20 keV.

3.2. *Diffraction effects*

The crystalline nature of the diodes causes non-negligible distortions in the EXAFS signal as a result of diffraction peaks: part of the incident X-ray beam is diffracted by crystallographic planes and this causes abrupt changes in the absorption coefficient and consequent distortions in the signal. As Fig. 3 (continuous line) shows, the shape and energy position of the Bragg reflections depend on the

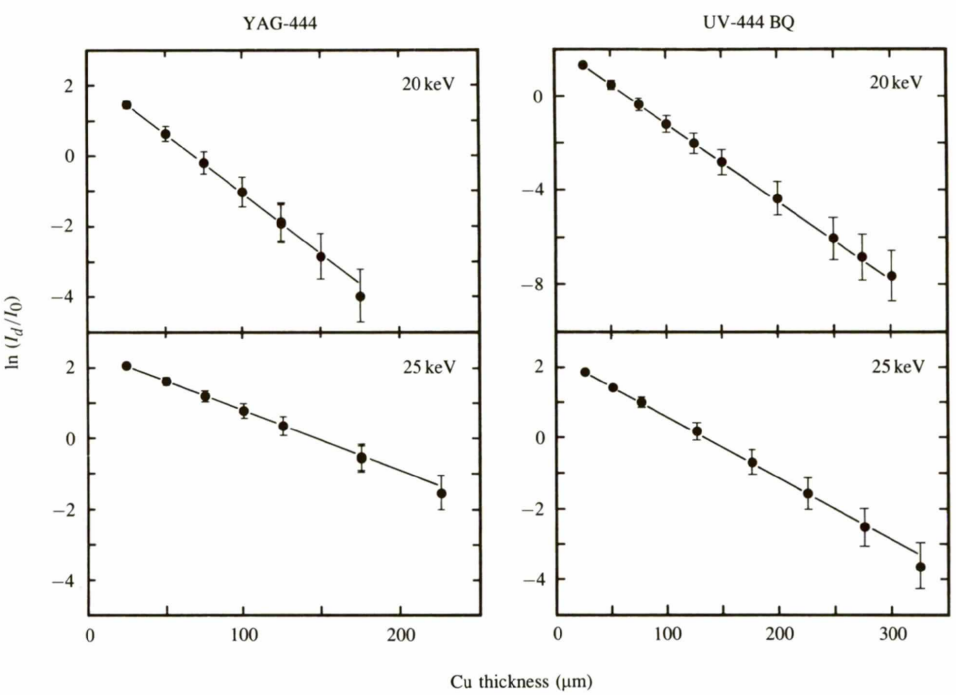

Figure 2
Linearity test of the diodes YAG-444 and UV-444BQ at 20 and 25 keV. I_0 and I_d are the current intensities measured before and after the absorbing Cu foils.

angle between the diode surface and the incident beam. In order to average the effects of diffraction we mounted the diode on a device able to tilt the diode surface continuously with respect to the beam direction. The optimal result was obtained by changing the orientation of the diode within a few degrees, at a frequency of 2 Hz. Figs. 3 and 4 show the I_0/I ratio obtained measuring the beam intensity I_0 with an ionization chamber and the transmitted signal I with stationary (continuous line) and rocking (dashed line) diode. These results show the effectiveness of this method: the diffraction peaks disappear because they are well averaged by rocking the diode. The motion of the diode does not change the average value of the measured current although it increases the intensity of its fluctuations: typically, a dark current value of *ca* 5.00 ± 0.05 pA for the fixed UV-444BQ diode becomes *ca* 5.0 ± 0.5 pA when the diode is rocking.

We have also checked if the rocking motion of the diode can perturb the EXAFS signal: comparative measurements using an ionization chamber (IC configuration) or a photodiode (PD configuration) as detector for the transmitted I signal have been made. To make a better comparison between these two detection schemes, we have calculated an average absorption S as a smooth function best fitting the ratio I_0/I, measured in absence of the sample, over the whole energy range; we have then calculated the ratio $\Delta S/S$ for every measured point as

$$\Delta S/S = (I_0/I - S)/S. \quad (2)$$

As Fig. 5 shows, the behaviour obtained for the $\Delta S/S$ ratios in the IC and PD configurations is similar: the increase of electrical noise connected to the movement of the diode is very low (the integration time was 1 s step^{-1}). The electrical noise could be further reduced by a more careful shielding of the electrical connections.

3.3. *EXAFS measurements and analysis*

A comparison between EXAFS spectra obtained measuring the transmitted signal with stationary or rocking diodes and an ionization chamber has been made at the K edges of Ge and Mo in the energy ranges 10.95–12.6 and 19.85–21.5 keV, respectively. All measurements were performed at room temperature. The EXAFS signals $\chi(k)$, where k

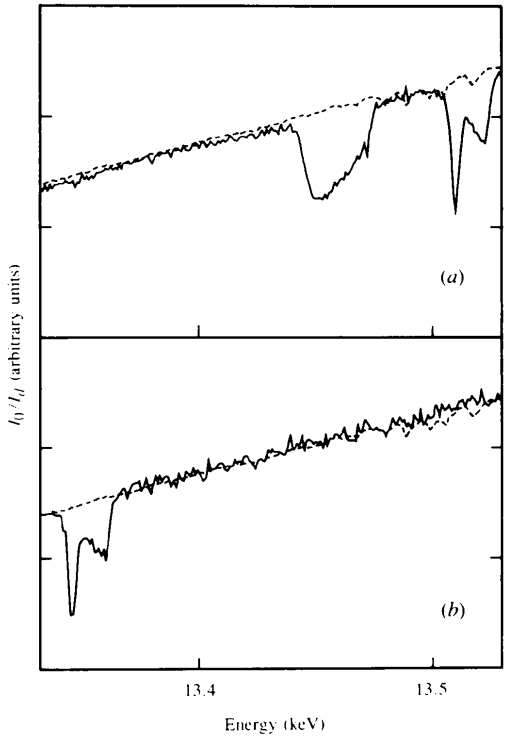

Figure 3
Example of diffraction effects from the diodes: (*a*) and (*b*) refer to different orientations of the diode with respect to the photon beam. I_0 and I_d are the current intensities measured, in the absence of the sample, by the ionization chamber and the UV-444BQ diode placed at *ca* 40 cm behind the chamber, respectively. The continuous line refers to the stationary diode and the dashed line to the rocking diode.

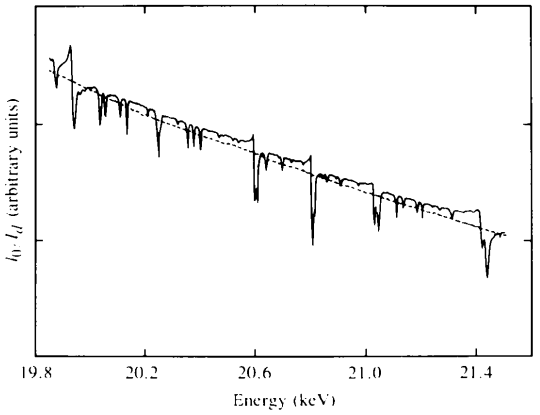

Figure 4
Influence of the diffraction effects in the energy range corresponding to EXAFS at the Mo K edge. As in Fig. 2, I_0 and I_d are the current intensities measured, in the absence of the sample, by the ionization chamber and the YAG-444 diode, respectively. The continuous line refers to the stationary diode and the dashed line to the rocking diode.

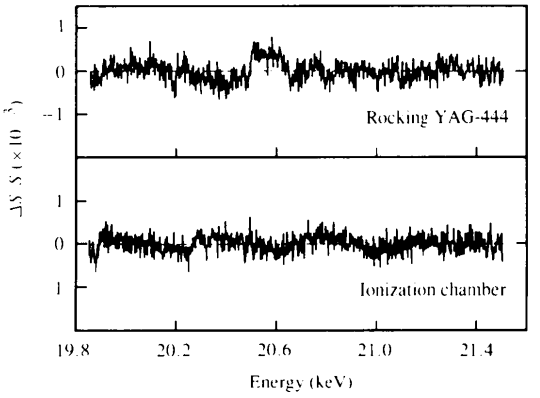

Figure 5
Signal-to-noise comparison for the IC and PD configuration using equation (2).

is the photoelectron wavevector, were extracted from the experimental spectra by conventional methods (Lee, Citrin, Eisenberger & Kincaid, 1981; Dalba, Fornasini & Rocca, 1993), and are shown in Figs. 5 and 7. In the fixed PD configuration the signal is perturbed by the presence of Bragg diffraction peaks; this is well illustrated in Fig. 6 where the EXAFS signals at the K edge of Mo are compared for the three different configurations (IC, fixed PD and rocking PD). The distortions due to Bragg diffraction peaks in the EXAFS signals of stationary diodes are eliminated when using the rocking diodes.

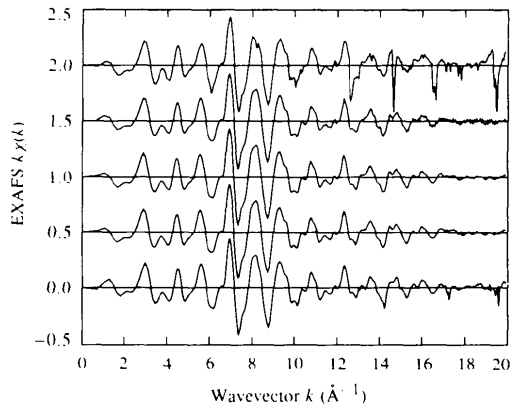

Figure 6
EXAFS signal at the Mo K edge obtained by using different detectors for the transmitted signal. From top to bottom: fixed and rocking UV-444BQ diode, ionization chamber, rocking and fixed YAG-444 diode.

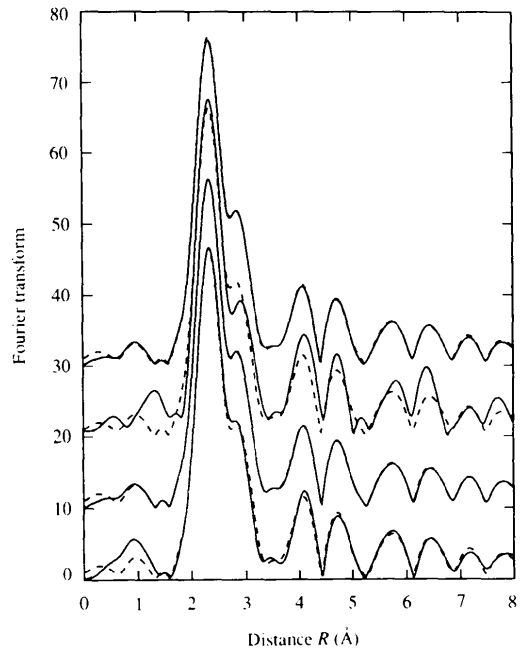

Figure 7
Fourier transforms of $k^3\chi(k)$ signals at the Mo K edge obtained using different detectors for the transmitted signal (Fourier transform range: 3.3–15 Å^{-1}, 10% Gaussian window). Continuous line, from top to bottom: rocking and fixed YAG-444 diode, rocking and fixed UV-444BQ diode; dashed line: ionization chamber.

The contributions to EXAFS of different coordination shells can be separated by a Fourier-filtering procedure. In Figs. 7 and 9 the Fourier transforms of the signals obtained in different detector configurations are compared. It is evident that the Fourier transforms obtained in the IC and rocking PD configurations are indistinguishable, while the Fourier transforms obtained in the fixed PD configuration are clearly different. Note that the Fourier transforms presented in Fig. 7 were performed in a reduced range: 3.3–15 Å^{-1}. By extending the Fourier transform range to 20 Å^{-1} the differences are strongly enhanced. However, even with the reduced range, the Fourier-transform signals show important differences.

A quantitative evaluation of the differences between structural parameters determined from EXAFS signals measured by different detection schemes has been attempted by separately analyzing phases and amplitudes of the first-shell Fourier-filtered EXAFS signals by the ratio method (Lee *et al.*, 1981; Dalba *et al.*, 1993).

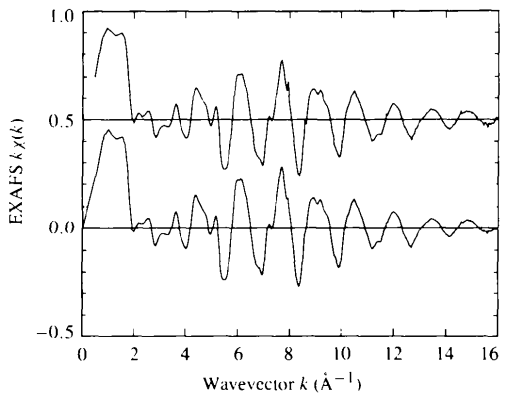

Figure 8
EXAFS signal at the Ge K edge obtained using the rocking UV-444BQ diode (top) and the ionization chamber (bottom) for monitoring the transmitted signal.

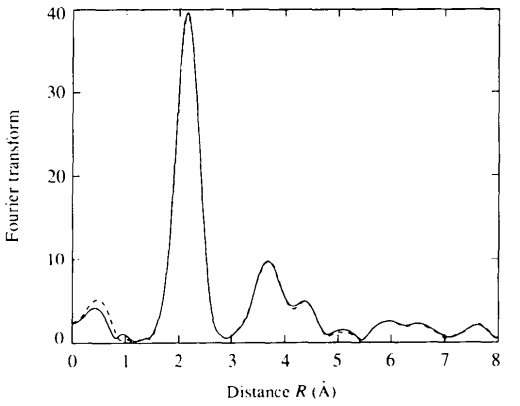

Figure 9
Fourier transforms of $k^3\chi(k)$ signals at the Ge K edge obtained using the rocking UV-444BQ diode (continuous line) and the ionization chamber (dashed line) as transmitted signal detectors. Fourier transform range: 2.7–16 Å^{-1}, 10% Gaussian window.

Phases and amplitudes of the first-shell EXAFS signals of Mo in the IC, rocking PD and fixed PD configurations were compared. Some details of the analysis are reported in Figs. 10 and 11, where the logarithm of the amplitudes ratio *versus* k^2 and the phase difference *versus* k are plotted together with the corresponding best-fitting straight lines. The intercept at $k = 0$ and the slope of the best-fitting straight line in Fig. 10 give the ratio of coordination numbers and the difference between the mean-square relative displacements (MSRDs), respectively; the slope of the best-fitting straight line in Fig. 11 gives the difference in interatomic distance. Note that in Figs. 10 and 11 we have plotted only the curves related to rocking PD configurations: in fact, the curves related to fixed PD configurations show oscillations five times higher, and would normally be rejected as unreliable. However, quantitative analysis with a best-fit procedure was performed for all the measured spectra of Mo. The results of the analysis are presented in Table 2. When analysing phase differences and amplitude ratios, the agreement between spectra measured by IC and rocking PD configurations can be considered satisfactory. The spectra measured by fixed PD configurations can still be considered satisfactory with respect to coordination number and interatomic distance; the difference in MSRD can, however, be non-negligible for high-accuracy studies because it is comparable with the absolute value of MSRD at room temperature. A better assessment of the quality of the data is obtained by analysing phase differences and amplitude ratios including lowest order anharmonic terms, *e.g.* the cumulants C_4 and C_3 (Dalba *et al.*, 1993), and checking the stability of physical parameters against the increase of fitting parameters. When considering the results of the cumulant analysis in Table 2, the superiority of the rocking PD configuration with respect to the fixed PD configuration is evident: in the former only a slight increase of the MSRD difference is produced, while in the latter unacceptable variations of the coordination number are generated.

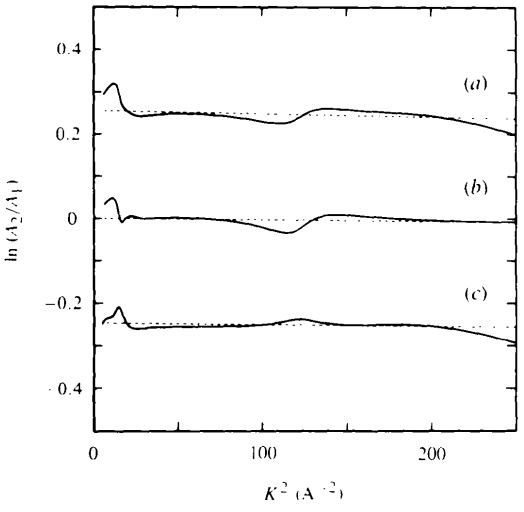

Figure 10
EXAFS of the first coordination shell of Mo: analysis of amplitudes. (*a*) A_1 = ionization chamber, A_2 = YAG-444; (*b*) A_1 = UV-444BQ, A_2 = YAG-444; (*c*) A_1 = UV-444BQ, A_2 = ionization chamber. The dashed lines are best-fit straight lines (harmonic approximation). Plots (*a*) and (*c*) have been vertically shifted by +0.25 and −0.25, respectively.

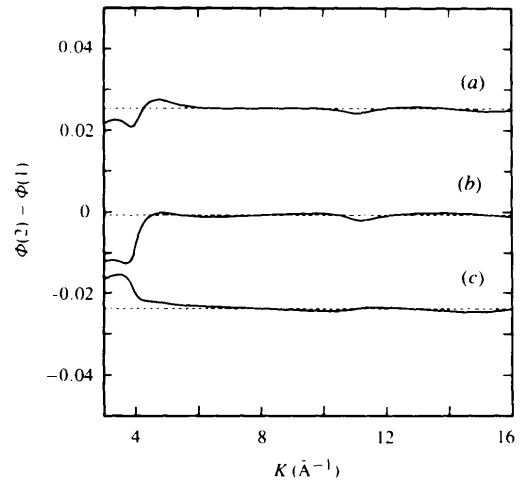

Figure 11
EXAFS of the first coordination shell of Mo: analysis of phases. (*a*) $\Phi(1)$ = ionization chamber, $\Phi(2)$ = YAG-444; (*b*) $\Phi(1)$ = UV-444BQ, $\Phi(2)$ = YAG-444; (*c*) $\Phi(1)$ = UV-444BQ, $\Phi(2)$ = ionization chamber. The dashed lines are best-fit straight lines (harmonic approximation). Plots (*a*) and (*c*) have been vertically shifted by +0.025 and −0.025 rad, respectively.

Such kinds of differences between rocking and fixed configurations could become crucial when studying more complex systems requiring a high signal-to-noise ratio.

4. Conclusions

This paper shows that it is possible to measure good EXAFS spectra with PIN silicon photodiodes by averaging the effect of diffraction peaks using a precession motion of the detector. The linearity of these detectors has been verified up to 10^{-6} A with synchrotron radiation at the SRS, Daresbury: the upper limit is being investigated at the ESRF, Grenoble, where a much higher photon flux is provided. If the efficiency of currently used ionization chambers must be reduced (by lowering the gas pressure) in order to avoid saturation at high photon fluxes, PIN diodes can provide comparable results with good signal-to-noise ratio and stability. A significant limit of the PIN silicon detectors tested in this work is the reduced efficiency at energies higher than 10 keV because of the small thickness of the effective depletion layer. Work is in progress to measure the effective depletion layer of Si photodiodes with X-ray beams of different energies and to test the use of PIN detectors based on materials with higher absorption coefficients.

The authors wish to thank E. Burattini and the staff of PWA Laboratory in Frascati (Rome, Italy). The help

Table 2
Quantitative analysis of first-shell EXAFS of Mo carried out by the ratio method.

The reference spectrum is that measured by the IC configuration. For both diodes the rocking and fixed configurations are compared. The phase and amplitude analyses were performed in harmonic approximation (linear) as well as including the first-order anharmonic contributions, cumulants C_3 and C_4. The best fit was obtained in the range 5–15 Å^{-1} for amplitude and 6–15 Å^{-1} for phase analysis.

		N/N_{IC}	$\Delta\sigma^2$ (Å^2)	ΔC_4 (Å^4)	ΔR (Å)	ΔC_3 (Å^3)
UV-444BQ	Rocking	1.00	$<1 \times 10^{-6}$		-1×10^{-3}	
	Fixed	1.06	2.2×10^{-3}		-1×10^{-3}	
	Rocking	1.02	1.7×10^{-4}	2×10^{-6}	-2×10^{-3}	-6×10^{-6}
	Fixed	1.14	-1×10^{-3}	1×10^{-5}	3×10^{-3}	4×10^{-5}
YAG-444	Rocking	0.98	5×10^{-5}		-1×10^{-3}	
	Fixed	1.01	5×10^{-5}		1×10^{-3}	
	Rocking	0.98	6×10^{-5}	2×10^{-7}	-1×10^{-3}	-4×10^{-6}
	Fixed	0.57	-6×10^{-3}	-8×10^{-5}	-1×10^{-3}	-2.9×10^{-5}

and assistance of J. Worgan and B. Dobson during the measurements at the SRS (Daresbury, UK) are greatly acknowledged.

References

Bevington, P. R. (1969). *Data Reduction and Error Analysis for the Physical Sciences*. New York: McGraw-Hill.

Bouldin, C. E., Forman, R. A. & Bell, M. I. (1987). *Rev. Sci. Instrum.* **58**, 1891–1894.

Dalba, G., Fornasini, P. & Rocca, F. (1993). *Phys. Rev. B*, **47**, 8502–8514.

Goulon, J. (1991). *Proceedings of the European Workshop on X-ray Detectors for Synchrotron Radiation Sources*, Aussois, France, edited by A. H. Walenta, pp. 39–50. ZESS, Center for Sensor Systems, University of Siegen, Germany.

Lagarde, P., Lemonnier, M. & Dexpert, H. (1989). *Physica B*, **158**, 337–338.

Lee, P. A., Citrin, P. H., Eisenberger, P. & Kincaid, B. M. (1981). *Rev. Mod. Phys.* **53**, 769–806.

Pant, J. & Hayes, T. M. (1994). *Rev. Sci. Instrum.* **65**, 3389–3392.

Storb, C., Dedek, U., Weber, W. & Lengeler, B. (1991). *Nucl. Instrum. Methods Phys. Res.* A**306**, 544–548.

Wilkinson, D. H. (1950). *Ionization Chambers and Counters*. Cambridge University Press.